Computational Fluid Dynamics JOURNAL 13(4):93 January 2005 (pp.714–721)

Selected Papers Presented at Fifth Asian Computational Fluid Dynamics Conference held on October 27-30, 2003 at Busan, Korea

APPLICATIONS OF STOKES EIGENFUNCTIONS TO THE NUMERICAL SOLUTIONS OF THE NAVIER-STOKES EQUATIONS IN CHANNELS AND PIPES

Bernd RUMMLER †

Abstract

General classes of boundary-pressure-driven flows of incompressible Newtonian fluids in three-dimensional (3D) channels and in 3D pipes with known steady laminar realizations are investigated respectively. The characteristic physical and geometrical quantities of the flows are subsumed in the kinetic Reynolds number Re and a parameter ψ, which involves the energetic ratio and the directions of the boundary-driven part and the pressure-driven part of the laminar flow.
We prescribe periodical conditions in the unbounded directions for the deviation $\mathbf{u}$ from the scaled laminar velocity $\boldsymbol{u}_L$. The solution of non-stationary dimension-free Navier-Stokes equations is sought in the form $\underline{\boldsymbol{u}} = \boldsymbol{u}_L + \boldsymbol{u}$, where the initial conditions are taken as small perturbations of $\boldsymbol{u}_L$. We receive out of the dimension-free Navier-Stokes equations for $\boldsymbol{u}$ - by the use of the Galerkin method - autonomous systems (S) of ordinary differential equations for the time-dependent coefficients of the spatial Stokes eigenfunction. The numerical investigations of the systems (S) for various geometries, initial conditions, Reynolds number Re and parameters ψ show significant effects and essential details in the transition from laminar to turbulent flows. Especially we get hints for the mechanism of bifurcation and good results for the critical Reynolds number as well as for the mean velocities.

Key Words: Navier-Stokes equations, Stokes eigenfunctions, Galerkin methods, Transition to turbulence

1 Introduction

The channel flow and the pipe flow of incompressible Newtonian fluids are well known as old-established objects of preference in theoretical and applied fluid-dynamic research. Owing to the simple geometry of the domains - these flows are ideal qualified for studies to the transition to turbulence and for investigations to extract further deterministic features from a random, fine-grained turbulent flow (cf.[1-5]).

It is the purpose of our investigations to check and to clarify the possibilities of using low-dimensional Galerkin spaces defined by Stokes eigenfunctions for fact finding of the mechanism of the transition to turbulence in the non-stationary 3D-Navier-Stokes equations (NSE). Particularly, our studies are targeted on the behavior of such approximations in the vicinities of critical Reynolds numbers.

We explore a general class of scaled flows of incompressible Newtonian fluids in unbounded channels and in unbounded pipes in $\boldsymbol{R}^3$, which can be described by the sum of laminar boundary-driven Couette (angular momentum for pipes) flow $\boldsymbol{u}_{L,c}$, of laminar pressure-driven Poiseuille flow $\boldsymbol{u}_{L,p}$, and of a time-dependent part $\boldsymbol{u}$. The first and second addenda

Received on November 27, 2004.

† Institute for Analysis und Numerics, Otto-von-Guericke-University Magdeburg PF 4120, D-39016 Magdeburg, Germany TEL: +49-391-6712236 Fax: +49-391-6718073 E-mail : bernd.rummler@mathematik.uni-magdeburg.de

are used to define the kinetic Reynolds number and a weighting parameter ψ for the energetic ratio and the direction of action of the boundary- and pressure-driven parts from $\boldsymbol{u}_L$. Low-dimensional approximation spaces spanned by the subsystems of Stokes eigenfunctions with periodic conditions in the former unbounded directions are applied for the direct numerical study of systems of Galerkin equations (cf.[5-10]).

The essential notations and governing equations supplemented with initial and boundary conditions are outlined in section 2. After convenient scaling we decompose the velocity fields $\underline{\boldsymbol{u}}(t,\boldsymbol{x})$ into the laminar flow $\boldsymbol{u}_L(\boldsymbol{x})$ and the remaining velocity $\boldsymbol{u}(t,\boldsymbol{x})$ (fulfilling homogeneous Dirichlet conditions on the boundary of the channel or on the boundary of the pipe): $\underline{\boldsymbol{u}} = \boldsymbol{u}_L + \boldsymbol{u}$. Additionally, periodic conditions in former unbounded directions are required for $\boldsymbol{u}$. The pressure is decomposed similarly. The kinetic Reynolds numbers and a weighting parameter ψ for the energetic ratio and the direction of action of the boundary- and pressure-driven parts of $\boldsymbol{u}_L$ are also defined in this section.

We explain the Stokes operator and the Galerkin approximation $\boldsymbol{u}_N := \sum_{j=1}^{N} g_j \boldsymbol{w}_j$ of the so-called weak solutions ([11],[12]) $\boldsymbol{u}$ of the NSE for the remaining velocities in section 3, where the $\{\boldsymbol{w}_j\}_{j=1}^{\infty}$ are the Stokes eigenfunctions. The Galerkin equations (as an autonomous system of ordinary differential equations for the coefficients $g_j(t)$ of the eigenfunctions $\{\boldsymbol{w}_j(\boldsymbol{x})\}_{j=1}^{N}$) are stated there.

Section 4 is devoted to the numerical method and the results. At first a fixed period $2{\cdot}l = 2{\cdot}2.69$ was chosen for historical reasons (cf. [13]). With this choice is the dimension of the Galerkin space $N(\lambda) = N(\lambda_{max})$ determined by a bound λ_{max} for the eigenvalues λ. λ_{max} is taken in such a way, that the Galerkin space includes two significant modes for the modification of the mean velocity both for the pure Couette-flow and the pure Poiseuille-flow. For the calculation of the coefficients in forming the system (S) are used universalized tools of combined C- and MAPLE-routines together with implemented rules of general addition theorems in form of allocation-lists.

The corresponding systems of ordinary differential equations were solved numerically for several values of the parameters Re, ψ and a set of initial values $\{g_j(0)\}, j = 1, ..., N$ (small $\boldsymbol{u}_{N,(0)} := \sum_{j=1}^{N} g_j(0)\boldsymbol{w}_j$), where the kinetic energy $E(t) := \sum_{j=1}^{N} g_j^2(t)$ of the Galerkin approximations $\boldsymbol{u}_N$ was used as a measure of turbulence.

2 The Basic Notations and Equations

The non-stationary NSE describe the evolution in time of an incompressible Newtonian fluid. We are interested on the channel flow and on the pipe flow, which means, that the fluid is filling after scaling with R in [m] an open unbounded domain Ω in $\boldsymbol{R}^3$:

$$\Omega := \{R^{-1}\boldsymbol{y} = \boldsymbol{x} = (x_1, x_2, x_3)^T \in \boldsymbol{R}^3 : \sqrt{x_2^2 + \delta^* x_3^2} < 1\},$$

where $2R$ is the thickness of the channel (with $\delta^* = 0$) resp. the diameter of the pipe (with $\delta^* = 1$).

We use $v_{char} = R(c_c^2 + c_p^2)^{1/2}$ as the velocity scale, which results from the common known stationary laminar velocity fields $\boldsymbol{v}_L(R\boldsymbol{x})$:

$$\begin{aligned}\boldsymbol{v}_L(R\boldsymbol{x}) :=& Rc_c \cdot \underbrace{((1-\delta^*)x_2, -\delta^* x_3, \delta^* x_2)^T}_{=\boldsymbol{u}_{L,c}} \\ &+ Rc_p \cdot \underbrace{\chi(1-(x_2^2+\delta^* x_3^2), 0, 0)^T}_{=\boldsymbol{u}_{L,p}} \\ =& \boldsymbol{v}_{L,c} + \boldsymbol{v}_{L,p},\end{aligned}$$

where c_c, c_p are velocity parameters in [1/s] and χ is chosen in such a way that for $c_c = c_p$ the velocity fields $\boldsymbol{v}_{L,c}$ and $\boldsymbol{v}_{L,p}$ result the equal kinetic energy in a control volume.

We establish the parameter $\psi \in [0, 2\pi)$ for all $\boldsymbol{v}_L \neq \boldsymbol{0}$ as an indicator for the energetic ratio and the direction of action of the parts of the laminar velocity by:

$$\begin{aligned}\cos\psi &:= c_c(c_c^2 + c_p^2)^{-1/2} \\ \sin\psi &:= c_p(c_c^2 + c_p^2)^{-1/2}\end{aligned}$$

We explain the *kinetic* Reynolds number Re by $Re = Re(c_c, c_p) := \frac{R^2}{\nu}(c_c^2 + c_p^2)^{1/2}$, the time scale $\frac{R^2}{\nu}$ and the scale for the kinematic pressure as $\nu(c_c^2 + c_p^2)^{1/2}$; where ν denotes the kinematic viscosity in $[m^2/\mathrm{s}]$.

The velocities and pressures are handled by the use of splitting up formulas:

$$\underline{\boldsymbol{u}} = \boldsymbol{u}_L + \boldsymbol{u} = \cos\psi\, \boldsymbol{u}_{L,c} + \sin\psi\, \boldsymbol{u}_{L,p} + \boldsymbol{u}$$

and

$$\underline{p} = p_L + p = \cos\psi\, p_{L,c} + \sin\psi\, p_{L,p} + p,$$

where $\boldsymbol{u}_L$ and p_L are the scaled laminar fields.

Finally periodic conditions for $\boldsymbol{u}$ and p are required instead of conditions in infinity: **(P):**

$$\boldsymbol{u}(t,x_1,x_2,x_3) = \boldsymbol{u}(t,x_1+2l,x_2,x_3+2l(1-\delta^*))$$
$$p(t,x_1,x_2,x_3) = p(t,x_1+2l,x_2,x_3+2l(1-\delta^*))$$

The initial-boundary value problem for the unknowns $\boldsymbol{u}(t,\boldsymbol{x})$ and $p(t,\boldsymbol{x})$ is given by:

Problem 1: We seek solutions $\boldsymbol{u}(t,\boldsymbol{x})$ and $p(t,\boldsymbol{x})$ fulfilling:

$$\frac{\partial \boldsymbol{u}}{\partial t} - \triangle_{\boldsymbol{x}}\boldsymbol{u} + Re\Big(\sum_{j=1}^{3} u^j D_j \boldsymbol{u} + \sum_{j=1}^{3} u_L^j D_j \boldsymbol{u} + \sum_{j=1}^{3} u^j D_j \boldsymbol{u}_L\Big) + \nabla_{\boldsymbol{x}} p = \boldsymbol{0} \quad ,$$

$$(\text{with } D_j := \partial./\partial x_j, \quad j = 1,2,3\,),$$
$$\nabla_{\mathbf{x}} \cdot \boldsymbol{u} = 0 \qquad \text{in} \quad (0,T)\times\Omega$$
$$\boldsymbol{u}(0,\boldsymbol{x}) = \boldsymbol{u}_0(\boldsymbol{x}) \quad = \quad \underline{\boldsymbol{u}}(0,.) - \boldsymbol{u}_L(.)$$
$$\boldsymbol{u}(t,x_1,x_2,x_3)_{|(x_2)^2+\delta^*(x_3)^2=1} = \boldsymbol{0}, \quad \text{and} \quad \textbf{(P)}$$

3 Explanation of the Galerkin Approximations

We restrict the domain $\boldsymbol{\Omega}$ on the open bounded subdomain T_l considering the presupposed periodic conditions **(P)**:

$$T_l := \{\boldsymbol{x} \in \boldsymbol{\Omega} : \boldsymbol{x} = (x_1,x_2,x_3)^T;\ |x_1|,\ (1-\delta^*)|x_3| < l\},$$

in which we suppose $l \geq 1$.

It is convenient to use suitable function spaces in the mathematical treatment of Problem 1. Let us call these spaces $\boldsymbol{S} \subset (L_2(T_l))^3$ and $\boldsymbol{S}^1 \subset (W_2^1(T_l))^3$ (cf. [6], [9], [11]). The advantage of these spaces is, that their elements are solenoidal fields und fulfill the boundary conditions in a general sense. One can use the eigenfunctions $\{\boldsymbol{w}_j(\boldsymbol{x})\}_{j=1}^{\infty}$ of the Stokes operator $\boldsymbol{A}$ to span the spaces $\boldsymbol{S}$ and $\boldsymbol{S}^1$, where one can understand the Stokes operator as a stationary version of Problem 1 with $Re = 0$. Additionally we note that the Stokes operator is an operator with a pure point spectrum with real eigenvalues $\lambda_j > 0$ of finite multiplicity (cf. [6], [11-12]). We apply the associated eigenfunctions $\{\boldsymbol{w}_j(\boldsymbol{x})\}_{j=1}^{\infty}$ of the Stokes operator $\boldsymbol{A}$ (counted in multiplicity) for the explanation of the Galerkin approximations.

Let $(.,.)$ be the scalar product on $(L_2(T_l))^3$. We denote the number of eigenvalues of $\boldsymbol{A}$ with $\lambda_j \leq \lambda$ by $N = N(\lambda)$ and define the Galerkin space $\boldsymbol{M}_N$ as the span of $\{\boldsymbol{w}_1, \boldsymbol{w}_2, ..., \boldsymbol{w}_N\}$ in $\boldsymbol{S}$.
We explain the Galerkin approximation $\boldsymbol{u}_N(t,\boldsymbol{x}) := P_N u(t,\boldsymbol{x}) = \sum_{j=1}^{N} g_j(t)\boldsymbol{w}_j(\boldsymbol{x})$ [, with $g_j(t) := (\boldsymbol{u}(t,\boldsymbol{x}), \boldsymbol{w}_j)$, $j = 1,...,N,$] of the so-called weak solution $\boldsymbol{u}(t,\boldsymbol{x})$ of Problem 1 by:

Problem 2 Let the initial-value $\boldsymbol{u}_0$ be an element of $\boldsymbol{S}$. We seek a function $\boldsymbol{u}_N \in C^1(0,T,\boldsymbol{M}_N)$ such that for all $j \in \{1,\ldots,N\}$:

$$\frac{d}{dt}(\boldsymbol{u}_N, \boldsymbol{w}_j) + (\nabla \boldsymbol{u}_N, \nabla \boldsymbol{w}_j) + Re\{b(\boldsymbol{u}_N, \boldsymbol{u}_N, \boldsymbol{w}_j) + b(\boldsymbol{u}_L, \boldsymbol{u}_N, \boldsymbol{w}_j) + b(\boldsymbol{u}_N, \boldsymbol{u}_L, \boldsymbol{w}_j)\} = 0,$$
$$\boldsymbol{u}_N(0) \quad = \quad P_N \boldsymbol{u}_0\,,$$

where we have used the abbreviation $b(\boldsymbol{u},\boldsymbol{q},\boldsymbol{s}) := (\sum_{k=1}^{3} u^k D_k \boldsymbol{q}, \boldsymbol{s})$ for the trilinear-form, which is antisymmetric in relation to permutation of $\boldsymbol{q}$ and $\boldsymbol{s}$.

The Problem 2 is equivalent to the solution of the initial-value problem of an autonomous systems **(S)** of ordinary differential equations for the time-dependent (Galerkin-)coefficients $g_j(t)$ with the initial-values $g_j(0)$ for $j = 1,...,N$:

$$\frac{dg_j(t)}{dt} =: \dot{g}_j = -\lambda_j g_j - Re\Big(\sum_{i,s=1}^{N} b_{j,i,s} g_i g_s + \cos\psi \sum_{i=1}^{N} q_{j,i}^I g_i + \sin\psi \sum_{i=1}^{N} q_{j,i}^{II} g_i + \cos\psi \sum_{i=1}^{N} r_{j,i}^I g_i + \sin\psi \sum_{i=1}^{N} r_{k,i}^{II} g_i\Big),$$
$$j = 1,2,...,N\,, \quad \textbf{(S)}$$

$$g_j(0) = g_{j,0} := (\boldsymbol{u}_{(0)}(\boldsymbol{x}), \boldsymbol{w}_j),\ j = 1,2,...,N,$$

with

$$b_{j,i,s} := b(w_i, \boldsymbol{w}_s, \boldsymbol{w}_j) \quad (= -b_{s,i,j}),$$
$$i,j,s = 1,2,...,N\,,$$

$$q_{j,i}^I := b(\boldsymbol{w}_i, \boldsymbol{u}_{L,c}, \boldsymbol{w}_j)\,, r_{j,i}^I := b(\boldsymbol{u}_{L,c}, \boldsymbol{w}_i, \boldsymbol{w}_j)$$
$$(= -r_{i,j}^I),$$
$$q_{j,i}^{II} := b(\boldsymbol{w}_i, \boldsymbol{u}_{L,p}, \boldsymbol{w}_j)$$

$$r^{II}_{j,i} := b(\boldsymbol{u}_{L,p}, \boldsymbol{w}_i, \boldsymbol{w}_j)\,(= -r^{II}_{i,j})\,, \quad i,j = 1,2,...,N$$

One can understand the Galerkin approximation by the use of the eigenfunctions of the Stokes operator $\boldsymbol{A}$ as a Helmholtz projection on solenoidal vector fields. These Helmholtz projection generates a projection error, from what follows that the pressure p and the Galerkin approximations $p_{\widehat{N}}$ of the pressure p are in the kernel of the projection. It is possible to reconstruct the Galerkin approximations $p_{\widehat{N}}$ and the pressure p itself by the solution of an inhomogeneous Poisson equation. We note, that $p_{\widehat{N}}$ is calculable as a function of the solutions $g_j(t)$, $j = 1,...,N$, of **(S)** in the form of Fourier coefficients in the eigenfunctions of the scalar Laplacian with homogeneous Neumann conditions and in harmonic pressures resulting in the harmonic pressure gradient parts of the Stokes eigenfunctions.

4 Numerical Experiments and Results

The first part in the numerical treatment of our problem is the generation of the autonomous systems of ordinary differential equations **(S)**.

One has to fix the kind of flow (channel flow or pipe flow), the period l and after that an upper bound λ for the eigenvalues - respectively $N = N(\lambda)$ as the dimension of the Galerkin space.

Under these assessments of default parameters are the Stokes eigenfunctions $\{\boldsymbol{w}_j(\boldsymbol{x})\}_{j=1}^{N}$ generated by Maple preprocessing tools. These eigenfunctions are used as input parameters for universalized tools of combined C- and MAPLE-routines together with implemented rules of general addition theorems in the form of allocation-lists in the generation of the coefficients of the system **(S)** of ordinary differential equations. The result of the preprocessing work is a binary list of data (coefficients) representing the N equations of the system **(S)**.

The main step in the numerical treatment of the Galerkin approximations of the Navier-Stokes equations are studies of the numerical solutions of the systems **(S)** in the dependence of the energetic Reynolds number Re, the control parameter ψ and the initial values $g_j(0) := g_{j,0}\,\forall j = 1,2,...,N$, as free parameters.

Sometimes we will use the notation $\underline{g}(0)$ for the vector of the initial values $[g_1(0), g_2(0), ..., g_N(0)]^T$

We note that the initial values $g_j(0) := g_{j,0} = 0$, $\forall j = 1,2,...,N$, (resp. $\underline{g}(0) = \underline{0}$) stand for the scaled laminar velocities $\boldsymbol{u}_L$ as initial values of the Navier-Stokes systems.

We have applied Dormand-Price methods (DOPRI5) and Runge-Kutta-Fehlberg (RKF45) methods (cf. [14]) with step size control for the numerical solution of the systems **(S)**.

From a physical point of view, one can understand the small initial values $g_{j,0}$ for all $j = 1,....,N$ as small perturbations of the laminar flow at the time $t = 0$. (This agrees completely with experimental results where the laminar velocity field is also a realisation of the real flow in the domain of over-critical Reynolds numbers (e.g. if the walls are sufficiently smooth).) In other words, the initial conditions for the g_j have been chosen as small random values out of a ball of radius σ around the origin $\underline{0}$ in $\mathbf{R}^N$:

$B_\sigma(\underline{0}) := \{\underline{g}(0) \in \mathbf{R}^N : \sum_{j=1}^{N}(g_j(0) - 0)^2 = \sum_{j=1}^{N}(g_{j,0})^2 \leq \sigma^2\}$

If the initial conditions $g_{j,0}$ have a distance smaller than $\rho < \sigma$ from the origin in $\mathbf{R}^N$, where ρ depends on the Reynolds number Re and on the the parameter ψ, our numerical solutions of the autonomous systems of ordinary differential equations **(S)** tend to the zero of $\mathbf{R}^N$. The reason is the asymptotic stability of the laminar flow in the sense of Ljapunov. The radius ρ of this ball of asymptotic stability depends nearly exponentially on the Reynolds number Re.

Let us introduce the kinetic energy $E(t)$ of the approximated remaining velocity by: $E(t) := \sum_{j=1}^{N}(g_j(t))^2$

The kinetic energy $E(t)$ was elected as the master indicator for the evaluation of the solutions in our studies. The behavior in time of $E(t)$ shows whether the solution of the systems **(S)** tends to the origin of $\mathbf{R}^N$ (asymptotic stability) or not ?

The numerical experiments were the following: The numerical solutions of the Galerkin equations were calculated for several intervals of time and a set of initial values for varying parameters Re and ψ. The properties of these solutions were studied with respect to the behavior of the kinetic energy $E(t)$. In this sense the kinetic energy $E(t)$ was also applied as an indicator-measure of turbulence or bifurcations.

In a second turn of studies, the numerical solutions were calculated for a set of parameters Re and ψ with fixed initial values chosen as random values out of

spherical shells around the origin of $\mathbf{R}^N$ and for fixed intervals of time.

The general behavior of the kinetic energies $E(t)$ of the solutions of the systems **(S)** observed as a function of the scaled time t is monotonic decreasing for initial values $\underline{g}(0)$ out of the ball of asymptotic stability with the radius $\rho = \rho(Re, \psi)$, which depends on the Reynolds number Re and the parameter ψ. The function $E(t)$ returns to zero in a finite interval of the time t in this case:

$E(t) \to 0$ for $t \to t_o - 0$ with $t_o \leq 3.2$ - and $E(t)$ is equal to zero for all t with $t > t_o$.

The function $E(t)$ shows an aperiodic oscillating behavior for initial values $\underline{g}(0)$ chosen as values out of spherical shells with a radius σ at $\sigma > \rho(Re, \psi)$. There exists for all over-critical Re and all ψ (with the exception of $\psi = 0$ and $\psi = \pi$ in the pipe flow) positive constants $e = e(Re, \psi) > 0$ and $\widehat{e} = \widehat{e}(Re, \psi) > 0$ such that $\widehat{e} > E(t) > e$ nearly independent of the initial kinetic energy $E(0)$. The long-time behavior of the solutions in $E(t)$ is also governed by $\widehat{e}$ and e in the same way.
We remark that this statement is true for the channel flows in general. But it is also worth to explain the exceptions $\psi = 0$ and $\psi = \pi$ for pipe flows in detail:

For pipe flows is the critical Reynolds number $Re = Re_{crit.} \approx \infty$ at $\psi = 0,\ \pi,\ 2\pi$. (These are the cases of pure Couette flows.) So are values of ψ out of a vicinity of these numbers ($\psi = 0,\ \pi,\ 2\pi$) for pipe flows the sole exception, where our statement does not apply. We reemphasize that $\psi = 0,\ \pi,\ 2\pi$ stand for the pure boundary-driven Couette (angular momentum) pipe flow and $\psi = \pi/2,\ 3\pi/2$ stand for the pure pressure-driven Poiseuille flow in pipes.

Our numerical investigations provide good agreements with experimental results for critical Reynolds numbers, when the initial values has been taken in the order of the magnitude of physical perturbations (the perturbation-radius σ).

Especially we have got the critical Reynolds numbers for the border cases of the general pipe flows:

$$Re_{crit.}^{COUETTE} \approx \infty, \quad Re_{crit.}^{POIS.} \in (1400, 20000)$$

and the critical Reynolds numbers for the Couette flows and for the Poiseuille flows in channels:

$$Re_{crit.}^{COUETTE} \in (360, 500) \quad Re_{crit.}^{POIS.} \in (630, 900)\ .$$

Much to our surprise we found time periodic non-laminar solutions of a constant kinetic energy $E(t, Re)$ at fixed ψ-values out of a small ψ-interval ($\psi \approx \pi/6$) about a range of Reynolds numbers Re ($Re \in (1700, 6000)$) for pipe flows. In this case the rotation of the pipe acts stabilizing to the pressure-driven part of the velocity, like a bullet is stabilized by the spiral fluted barrel of a gun.

The time mean values of the coefficients of the remaining velocity field are defined by

$$\overline{g_j} := \frac{1}{T - t_0} \left(\int_{t_0}^{T} g_j(t)\, dt \right) \approx \frac{1}{n_1} \sum_{i=1}^{n_1} g_j(t_i)\,,$$
$$t_i \in [t_0, T]\,,\ j = 1, \ldots, N\,,$$

where n_1 is the number of Dormand-Price - resp. Runge-Kutta-Fehlberg time steps, t_i are the calculation points in time and t_0 is a time for which the kinetic energy starts to show an aperiodic oscillating behavior between an upper and lower level. The mean velocities are given for the general channel flow by

$$\begin{aligned} \overline{\underline{\boldsymbol{u}}}_N(x_2) &= \boldsymbol{u}_L(x_2) \\ &\quad + \frac{1}{2l \cdot 2l(T - t_0)} \int_{t_0}^{T} \int_{-l}^{l} \int_{-l}^{l} \boldsymbol{u}_N(t, \boldsymbol{x})\, dx_1\, dx_3\, dt \\ &\approx \boldsymbol{u}_L(x_2) + \sum_{i^\star \in I^\star} \overline{g_{i^\star}}\, \boldsymbol{w}_{i^\star}(\boldsymbol{x}), \end{aligned}$$

and for the general pipe flow by

$$\begin{aligned} \overline{\underline{\boldsymbol{u}}}_N(r) &= \boldsymbol{u}_L(r) \\ &\quad + \frac{1}{4l\pi(T - t_0)} \int_{t_0}^{T} \int_{0}^{2\pi} \int_{-l}^{l} \boldsymbol{u}_N(t, \boldsymbol{x})\, dx_1\, d\varphi\, dt \\ &\approx \boldsymbol{u}_L(r) + \sum_{i^\star \in I^\star} \overline{g_{i^\star}}\, \boldsymbol{w}_{i^\star}(\boldsymbol{x}), \end{aligned}$$

where the sets of significant coefficients $I^\star$ are equal to the sets of indices of the Stokes eigenfunctions, which are pure functions of x_2 or of r respectively. It is worth noting that the time averages $\overline{g_{i^\star}}$ with $i^\star \in I^\star$ assume much larger values than the time averages of all the other coefficients $\overline{g_j}$.

The time averaged mean velocities $\overline{\underline{\boldsymbol{u}}}_N(x_2)$ are illustrated on the left hand side of Figure 1 for a set of parameters ψ ($\psi \in [0, \pi]$) at the Reynolds number $Re = 1500$ in comparison with the correspondent

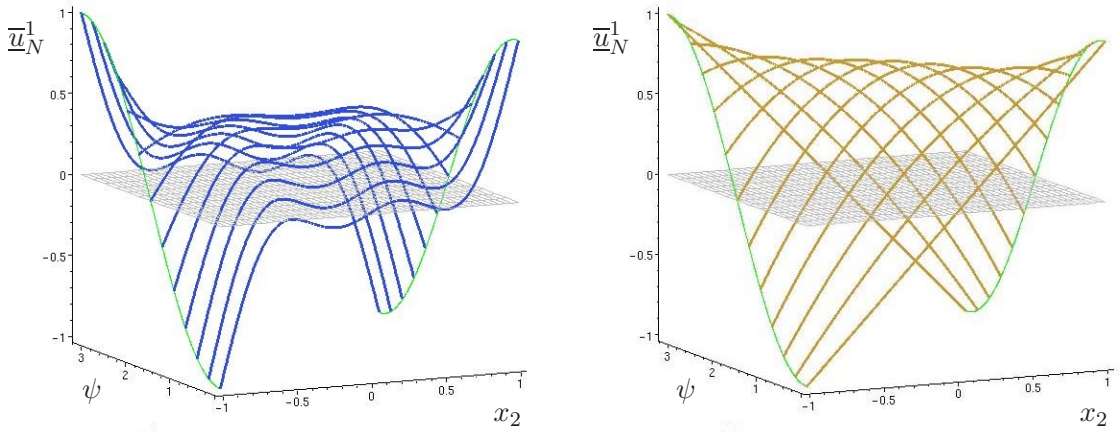

Fig.1: Behavior of the mean velocities $\overline{\underline{\boldsymbol{u}}}_N(x_2)$ in the channelfor $\psi \in [0, \pi]$ at $Re = 1500$ in comparison with the laminar velocities $\boldsymbol{u}_L$.

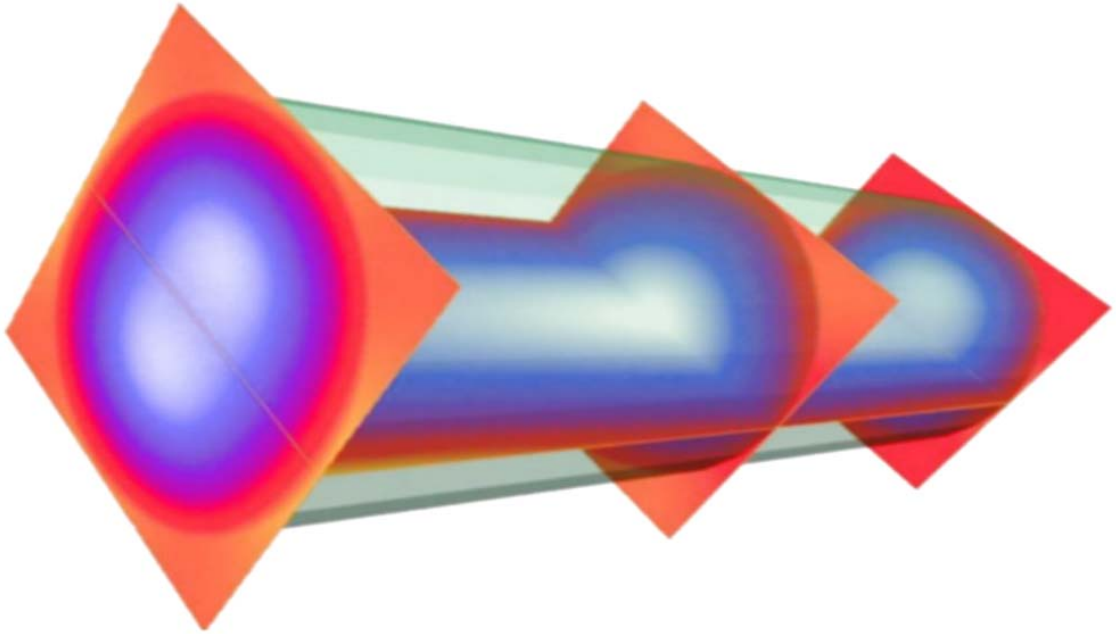

Fig.2: Kinematic pressure $\overline{\underline{p}}_{\widehat{N}}$ in a pipe flow at $Re = 1450$ and $\psi = \pi/4$.

laminar velocities $\boldsymbol{u}_L(x_2)$ on the right hand side of Figure 1. One can understand the change of the parameters ψ in Fig.1 in such a way that the flow starts as a pure Couette flow in the channel, passes the pure pressure-driven Poiseuille flow at $\psi = \pi/2$ and arrives the pure Couette flow at $\psi = \pi$, whereas the walls are moved in comparison with $\psi = 0$ with the same velocity but in the opposite direction.

The planes with $\overline{\underline{u}}^1_N(x_2) = 0$ and $(x_2, \psi) \in [-1, 1] \times [0, \pi]$ are displayed in Figure 1 as grey shaded planes in both graphical representations to give an opportunity to compare the mean velocities $\overline{\underline{u}}^1_N(x_2)$ with the laminar mean velocities $u^1_L(x_2)$ for fixed values of the parameter ψ. We note, that the non-physical regions of calculated backflows (cf. $\psi = 0$) are to understand in causal relationship to the well known Gibbs phenomenon at Fourier's series. Especially, one can regard the low-dimensional Galerkin spaces for our calculations as finite Fourier's series, including only two even modes and two odd modes for the correction of $\overline{\underline{u}}^1_N(x_2)$.

We have developed combined C- and MAPLE-

routines for the reconstruction of the scaled kinematic pressure $p_{\widehat{N}}$. In this routines is calculated $p_{\widehat{N}}(t,x)$ as a function of the solutions $g_j(t)$, $j = 1,...,N$, of the system **(S)** in the form of Fourier coefficients in the eigenfunctions of the scalar Laplacian with homogeneous Neumann conditions and in harmonic pressures resulting in the harmonic pressure gradient parts of the Stokes eigenfunctions.

The scaled kinematic pressure $\overline{\underline{p}}_{\widehat{N}} = p_L + p_{\widehat{N}}$ on cut planes through the scaled pipe is shown in the Figure 2. The kinematic pressure corresponds a pipe flow at a Reynolds number $Re = 1450$ and $\psi = \pi/4$. The boundary of the pipe is illustrated there as the green transparent surface. The scale for the kinematic pressure has been chosen from light blue (for large kinematic pressure) to red (for small kinematic pressure).

The agreement of our calculations with other experimental data for the root-mean-square values of the fluctuating velocities and the Reynolds stresses is less satisfactory. These results are to understand as a consequence of the Gibbs phenomenon again. We illustrate these quantities as examples in the Figures 3 and 4, where we have chosen to picture the calculations for a pure Poiseuille flow in a channel at $Re = 2217$ (and $\psi = \pi/2$).

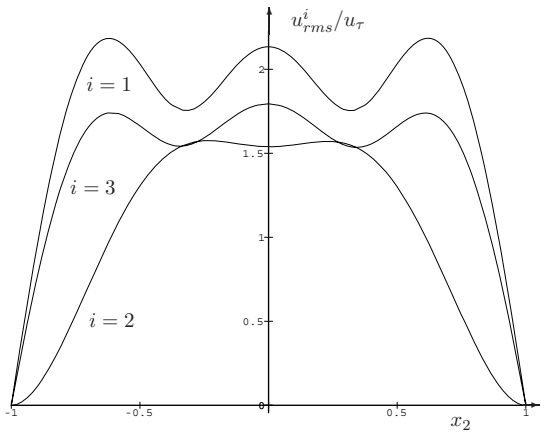

Fig.3: rms-values u^i_{rms}/u_τ, $i = 1,2,3$ in a channel flow at $Re = 2217$ and $\psi = \pi/2$.

5 Conclutions

We have proposed and discussed the application of Stokes eigenfunctions to the numerical solutions of the Navier-Stokes equations in this paper. The big advantage of these method consist in their nature. These method is derivable directly from the mathematical treatment of the Navier-Stokes equations.

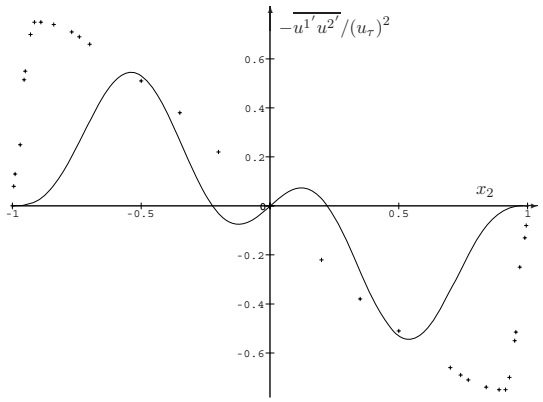

Fig.4: Calculated shear stress $-\overline{u^{1'}u^{2'}}/(u_\tau)^2$ in comparison with Eckelmann's [15] measurements (+ + +) in a channel flow at $Re = 2217$ and $\psi = \pi/2$.

From a physical point of view are the Stokes eigenfunctions to understand as the physical modes of a crawling flow, that means: the Stokes eigenfunctions are predestinated for the construction of the general solution-spaces of the Navier-Stokes equations. One has to note, that the use of such Stokes eigenfunctions is restricted to special geometries of the domains for the viscous flows - and special boundary conditions.

Currently, the available mathematical tools give the possibility to use the Stokes eigenfunctions explicit for (and in) the development of numerical tools for the calculation and investigastion of features for the channel flow and for the pipe flow of incompressible Newtonian fluids.

We have found that such tools are qualified for the determination of critical Reynolds numbers and also for investigations to the bifurcation behavior of solutions of the Navier-Stokes equations. The evaluation of our numerical investigations shows very good agreements with measurements for the transition from laminar to turbulent flows in the vicinity of the critical Reynolds numbers.

The direct calculations of the mean velocities, of the Reynolds stresses and of the root-mean-square values are less satisfactory, but due to the small dimension of our approximation space most probably.

However, one can hope to eliminate these disad-

vantages by the use of Galerkin spaces of a moderate larger dimension.

Finally it is to note, that our tools and investigations are able to provide substantial contributions to the mathematical understanding of transition to turbulent flows in channels and pipes.

REFERENCES

[1] Schlichting, H., Gersten, K., "Boundary Layer Theory", Springer (2000)

[2] Kim, J., Moin, P., Moser, R.D., "Turbulence statistics in fully developed channel flow at low Reynolds number", J.Fluid Mech., Vol.177, (1987), 133-166

[3] Bech, K.H., Tillmark, N., Alfredsson, P.H., Andersson, H.I., "An Investigation of turbulent plane Couette flow at low Reynolds numbers", J.Fluid Mech., Vol.286, (1995), 291-325

[4] Busse, F.,H., "Bounds on the Transport of Mass and Momentum by Turbulent Flow Between Parallel Plates", ZAMP (Vol. 20), (1969), 1-14

[5] Brosa, U., "Linear Analysis of Currents in a Pipe", Z.Naturforsch. 41a, (1986) 1141-1153

[6] Rummler, B., "Zur Lösung der instationären inkompressiblen Navier-Stokesschen Gleichungen in speziellen Gebieten", Magdeburg: Habilitation (1999/2000)

[7] Rummler, B., "The Eigenfunctions of the Stokes Operator in Special Domains I", ZAMM 77(1997) 8, 619-627

[8] Rummler, B., "The Eigenfunctions of the Stokes Operator in Special Domains II", ZAMM 77(1997) 9, 669-675

[9] Rummler, B., "Some Strange Numerical Solutions of the Non-stationary Navier-Stokes Equations in Pipes", in Math.& Math.Educ., World Scienific Publ. (2002), 264-280

[10] Batcho, P.F., Karniadakis, G.E., "Generelized Stokes Eigenfunctions: A New Trial Basis for the Solution of Incompressible Navier-Stokes Equations", J.Comp.Phys 115, (1994) 121-146

[11] Constantin, P., Foias, C., "Navier-Stokes Equations", Univ.of Chic.Press, Chicago (1988)

[12] Temam, R., "Navier-Stokes equations, theorie and numerical analysis" ,Amsterdam: North Holland (1979)

[13] ummler, B., Breitschuh, U., "Berechnung der turbulenten Couette-Strömung mittels Galerkinapproximation der Navier-Stokes-Gleichung - Ergebnisse und Probleme", ZAMM 64 (1984) 10, M 489-492

[14] Hairer, E., Norsett, S.P., Wanner, G., "Solving Ordinary Differential Equations I", Springer , Berlin ,(1993)

[15] Eckelmann, H., "Experimentelle Untersuchungen in einer turbulenten Kanalströmung mit starken viskosen Wandschichten", Mitt. MPI f. Strömungsforschung und AVA Göttingen Nr.48 (1970)